JACS
JOURNAL OF THE AMERICAN CHEMICAL SOCIETY
pubs.acs.org/JACS
Communication

# Nitrite Causes Nitrosative Stress to Iron Sulfur Clusters

Subhadeep Bera, Arijeet Ghude, Vincent J. Catalano, Jean-Marie Mouesca, Ricardo García-Serres,* and Leslie J. Murray*

Cite This: https://doi.org/10.1021/jacs.5c05636
Read Online
ACCESS | Metrics & More | Article Recommendations | Supporting Information

**ABSTRACT:** Nitric oxide (NO), produced by nitrite reductases or nitric oxide synthases, performs vital roles in signaling and the immune response. Iron sulfur (FeS) clusters are known targets for NO induced degradation, serving as sensors to trigger cellular responses. However, this FeS reactivity is proposed as NO specific, with no demonstrated reactivity toward nitrite, a soluble NO storage molecule. We demonstrate that synthetic FeS clusters supported by various ligands undergo facile nitrosylation by nitrite in the presence of a reductant, evidencing the nitrite reductase reactivity for FeS clusters. Moreover, a mononitrosylated $Fe_4S_4$ cluster, $[tempS_3Fe_4S_4(NO)]^{2-}$, can be readily synthesized by this approach, enabling further investigation into the FeS cluster repair and decomposition under NO induced oxidative stress.



Nitric oxide is a key gasotransmitter involved in immune response and inflammation[1−8] but has a short half-life due to rapid reactions with dioxygen, thiols, and metal cofactors.[9−11] Cells store NO in molecules like nitrite ($NO_2^-$), which can be reduced on-demnad to liberate NO (Figure 1A).[12−17] Heme cofactors in enzymes and synthetic model complexes facilitate nitrite reduction, forming a metal−NO adduct with net O atom transfer to a suitable acceptor (e.g., phosphines) or an oxo-metal complex with NO release.[18−23] Protein-bound iron−sulfur (FeS) clusters, such as $[Fe_4S_4]^{0/1+/2+}$, are susceptible to nitrosation by NO and subsequent cofactor dissociation, which are characteristics of nitrosative stress.[24] This sensitivity to NO has led to specific FeS proteins to be sensors to nitrosative stress and to trigger the cellular stress response.[25−40] Reaction of FeS clusters with NO results in rapid and uncontrolled nitrosation with mixtures of polynitrosyl species, including Roussin's black anion, Roussin's red ester, and dinitrosyl iron complexes (DNICs) observed (Figure 1B).[41−46] A mononitrosylated $Fe_4S_4$ species is proposed as the initial product of reaction with NO. This $[Fe_4S_4NO]$ cluster has remained elusive to characterization, however, with only one synthetic example in which sterically encumbering N-heterocyclic carbenes are used as ancillary ligands (Figure 2A).[47] Understanding the repair and downstream chemistry of nitrosylated FeS clusters has been consequently limited.[35,42,48−50]

Whereas heme and nonheme metal cofactors have known roles in nitrite to NO conversion, there has been no reported reactivity of FeS clusters toward nitrite. Holm and Weigel stated that nitrite is unreactive to a site differentiated 4Fe4S cluster with one chloride ligand, and LeBrun's group reported no reaction of $NO_2^-$ with the [4Fe-4S] NsrR holoprotein.[24,51] Herein, we demonstrate the general efficacy of nitrite as a NO source for $Fe_4S_4$ and $Fe_2S_2$ clusters using phosphines as sacrificial net O atom acceptors (Figure 2B). Use of a templating tris(phosphine) or tris(thiolate) ligand allows direct access to mononitrosylated $Fe_4S_4$ clusters, of which the thiolate congener is structurally characterized. Finally, the phosphine can be readily substituted for the NADH analogue (1)-benzyl-1,4-dihydronicotinamide (or BNAH) to effect nitrite to NO conversion, suggesting a broader role for nitrite in oxidative stress.

Complex $(Ph_4P)_2[(tempS_3)Fe_4S_4Cl]$ or $(Ph_4P)_2[\mathbf{1\text{-}Cl}]$ is readily derived from the reported $(Ph_4P)_2[(tempS_3)Fe_4S_4(SEt)]$ (Figures S1 and S14),[52] and confirmed as unreactive toward nitrite sources by NMR and IR spectroscopy (Figure S3).[24,51] Reaction of a stoichiometric equivalent of a phosphine and $(Ph_4P)NO_2$ in acetonitrile with $[\mathbf{1\text{-}Cl}]^{2-}$ results in complete conversion of the starting complex to a new species with pronounced new IR absorptions at 1682 $cm^{-1}$ and 1652 $cm^{-1}$ and $^{31}P$ NMR spectra support the corresponding phosphine oxide as a product (Figure S5). This IR absorption at 1682 $cm^{-1}$ is comparable to that of the assigned NO stretching mode of other metal nitrosyl species, including DNICs and the $[(IMes)_3Fe_4S_4(NO)]^{n+}$ ($n$ = 0−2) series of complexes (Figure 2A), and for a transient species observed by LeBrun and co-workers in reactions of $[(tempS_3)Fe_4S_4(SEt)]^{2-}$ with nitric oxide (ca. 1690 $cm^{-1}$).[47,53] The 1652 $cm^{-1}$ vibration is consistent with the tetra(nitrosyl) cluster, $[Fe_4S_4(NO)_4]^{2-}$. Other nitrite salts, such as $NaNO_2$, were tested and are competent for nitrosylation, but $(Ph_4P)NO_2$ allows easier separation of the chloride salt byproduct and minimizes the yield of $[Fe_4S_4(NO)_4]^{n-}$ (Figure S17A). Similarly, tris(cyclohexyl)phosphine afforded the maximal conversion of $(Ph_4P)_2[\mathbf{1\text{-}Cl}]$ to $(Ph_4P)_2[\mathbf{1\text{-}NO}]$ over the other phosphines tested (Figure S17B). The cluster, $(Ph_4P)_2[\mathbf{1\text{-}Cl}]$ is also unreactive toward phosphines, as noted

**Received:** April 2, 2025
**Revised:** June 3, 2025
**Accepted:** June 4, 2025

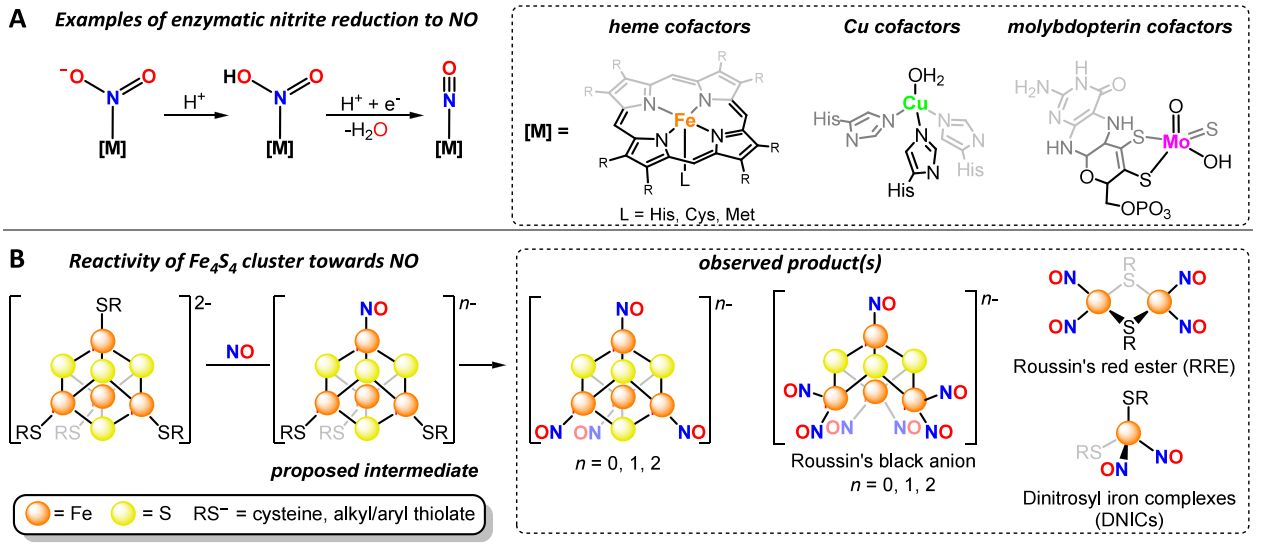


**Figure 1.** Nitrite reduction and NO generation by metallocofactors and reactivity of Fe−S clusters toward NO. General strategy utilized by enzyme cofactors to generate NO through nitrite reduction (A). Reactivity of FeS clusters toward NO proposed to proceed through a mononitrosyl $Fe_4S_4$ cluster, and subsequent nitrosylations to yield various possible products (B).

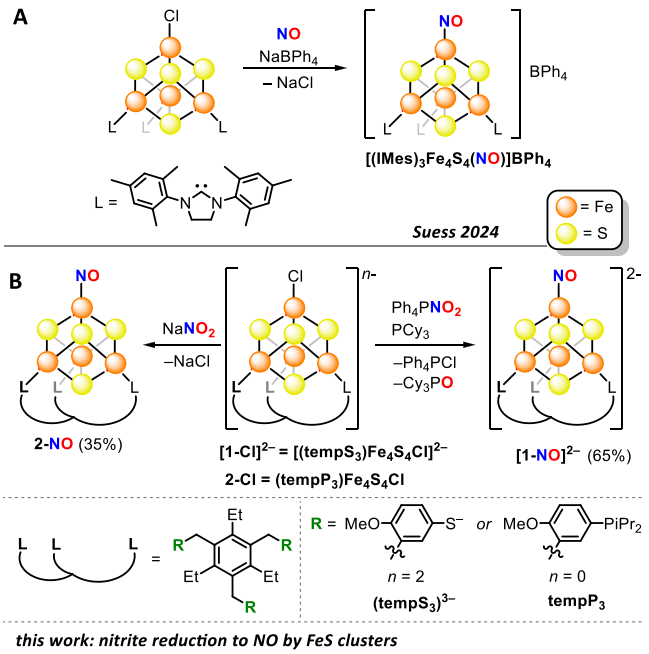


**Figure 2.** Prior example of a structurally characterized model of the 3:1 site-differentiated $[Fe_4S_4(NO)]^+$ cluster isolated by Suess and co-workers using NO and a sterically encumbering ligand (A) and the general pathway using nitrite reduction reported here (B).

for a related system,[51] and reaction of $PCy_3$ with nitrite in the absence of a cluster does not afford $Cy_3PO$ or any observable new product in $^{31}P$ NMR spectra (Figure S27).

Single-crystal X-ray diffraction analysis supports the product as $(Ph_4P)_2[(tempS_3)Fe_4S_4(NO)]$ or $(Ph_4P)_2$[**1-NO**] with a net substitution of $Cl^-$ by $NO^-$ based on charge balance within the lattice (Figure 3A). The unit cell contains two complexes with one having an Fe−N−O angle of 171.7(6)° (Figure 3B), and the other exhibiting positional disorder of the bound NO and refined in a 4:1 ratio with Fe−N−O angles of 153(2)° and 169(1)°, respectively (Figure S16). The Fe−N and N−O bond lengths agree with those of prior reported polynitrosyl iron complexes and for Suess's mononitrosyl $Fe_4S_4$ cluster,[46,47] all of which were accessed from NO. This cluster is asymmetric with one pair of Fe centers having a short iron−iron contact (i.e., 2.7013(9) Å and 2.7090(8) Å) and the other pair having a long iron−iron distance (i.e., 2.8145(9) Å and 2.783(1) Å), consistent with the coupled pairs of iron centers (i.e., two $Fe^{2.5+}_2$ or one $Fe^{2.5+}_2$ and one $Fe^{2+}_2$) invoked in DFT methods.[54]

To interrogate the electronic structure, Mössbauer spectra were recorded on [**1-NO**]$^{2-}$. Spectra recorded at 600 G and 5.6 K afford a broad, asymmetric doublet with an average isomer shift and quadrupole splitting ($\delta_{avg}$ = 0.45 mm/s, $\Delta E_{Qavg}$ = 1.14 mm/s) comparable to those of the starting chloride complex, [**1-Cl**]$^{2-}$ (Figure S1), and of protein-bound and other synthetic $[Fe_4S_4]^{2+}$ clusters.[55,56] Although the 600 G spectrum contains only one doublet, spectra recorded in 5 and 7 T applied magnetic fields require four distinct components to account for all absorptions and spectra best simulated with spin-Hamiltonian for an $S$ = 1 ground state (Figure 3C). The resulting spin-Hamiltonian fit parameters (Table S10) indicate one delocalized $Fe^{2.5+}Fe^{2.5+}$ pair and one partially localized $Fe^{2+}Fe^{u}$ pair, where $Fe^{u}$ denotes the site bearing the NO ligand. This analysis agrees with DFT calculations and prior conclusions on the $[(IMes)_3Fe_4S_4(NO)]^{n-}$ complexes (Figure 2A).[47] Whereas charge population analysis, which reflects electronic delocalization, and DFT computed Mössbauer isomer shifts suggest that $Fe^{2+}$ bound with NO is the most accurate description of the Fe−NO bond, the broken symmetry spin-coupling calculations implicate a triplet $NO^-$ donor antiferromagnetically coupled to a ferric center (Tables S11−S13). This ambiguity in describing the Fe−NO interaction highlights the precedented challenge of assigning formal metal oxidation states in metal NO adducts.

Given the ease with which nitrite and phosphines afford $(Ph_4P)_2$[**1-NO**], we examined the ligand donor atom type and cluster nuclearity on nitrite reduction. Starting with donor atom type, metalation of the triphosphine ($tempP_3$) ligand as for $(tempS_3)^{3-}$ affords $(tempP_3)Fe_4S_4Cl$ or **2-Cl**, as confirmed by X-ray crystallography (Figure S15) and Mössbauer spectroscopy (Figures S28, S29). **2-Cl** contains a formally


https://doi.org/10.1021/jacs.5c05636
J. Am. Chem. Soc. XXXX, XXX, XXX−XXX

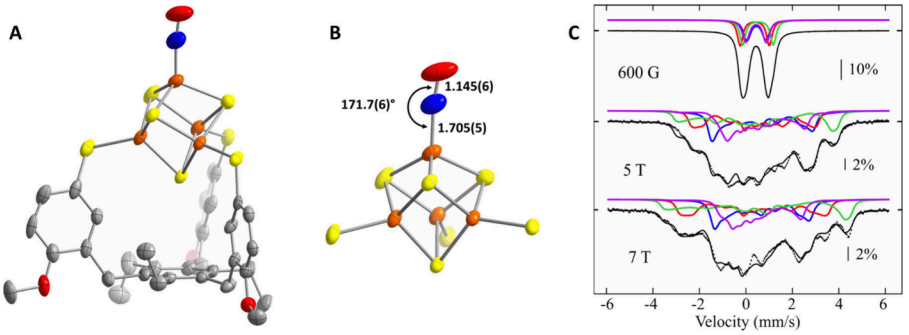


**Figure 3.** Characterization of $[\mathbf{1\text{-}NO}]^{2-}$. Solid state structure of $[\mathbf{1\text{-}NO}]^{2-}$ (A) and a detailed view of the cluster with the primary coordination sphere of the Fe centers and the bound NO depicted (B). Atoms are depicted as 50% probability thermal ellipsoids with orange, yellow, blue, red, and gray ellipsoids depicting Fe, S, N, O, and C, respectively. H atoms, two $Ph_4P^+$ counteractions, and solvent molecules omitted for clarity. Bond lengths are reported in Å. $^{57}$Fe Mössbauer spectra of $[\mathbf{1\text{-}NO}]^{2-}$ were recorded at 5.6 K with the magnetic field applied parallel to the $\gamma$ rays (C). Experimental points are plotted as vertical error bars. Colored lines correspond to the individual Fe sites of the cluster, with the black line superimposed with the experimental points being the composite spectrum obtained by summing individual spectra with the same integration. The fit parameters of the four colored lines are given in Table S10.

$[Fe_4S_4]^+$ cluster, which is one-electron more reduced than $[\mathbf{1\text{-}Cl}]^{2-}$.[55,57] Initial reactions of **2-Cl** with nitrite sources and phosphines generated the phosphine oxide of $tempP_3$ (i.e., $temp(PO)_3$) regardless of equivalents of $PCy_3$ added (Figures S10, S11).[58] The optimized reaction conditions based on IR and $^1$H NMR spectroscopy are **2-Cl** with one equivalent of $NaNO_2$ in a mixture of PhF and methanol (Figure S19). The major product complex exhibits solution-phase $C_{3v}$ symmetry in $^1$H NMR spectra, and a prominent IR absorption at 1717 $cm^{-1}$ (Figure S12), which together with combustion analysis, leads to our tentative assignment of **2-NO** as this major product. The $\nu_{NO}$ in **2-NO** is blue-shifted versus that in $[\mathbf{1\text{-}NO}]^{2-}$, despite the cluster being formally one-electron more reduced than in $[\mathbf{1\text{-}NO}]^{2-}$, and also higher in energy than that for $[(IMes)_3Fe_4S_4(NO)]$ from Suess and co-workers(cf. 1657 $cm^{-1}$).[47] Thus, thiolate ligands are the strongest donors of the series, accounting for almost one formal oxidation state of the $Fe_4S_4$ cluster, and suggests that synthetic FeS models using carbene or phosphine ligands will require more formally reduced clusters as compared to cysteine thiolate supported enzyme cofactors clusters to effect similar reactivity toward small molecules.[57,59−62] Reaction of $[Fe_4S_4Cl_4]^{2-}$ or $[Fe_4S_4(SEt)_4]^{2-}$ with 4 equiv of $[Bu_4N][NO_2]$ and of $PCy_3$ yielded $[Fe_4S_4(NO)_4]^{2-}$ based on the characteristic absorption at 1652 $cm^{-1}$ in IR spectra and the parent ion observed in ESI/MS data (Figures S22−S25).[63] Efforts to control the extent of nitrosylation had limited success; however, reaction of $[Ph_4P]_2[Fe_4S_4(SEt)_4]$ with 1 equiv of $[Bu_4N][NO_2]$ and of $PCy_3$ yields a product with an IR absorption of ∼1680 $cm^{-1}$, which is comparable to $[\mathbf{1\text{-}NO}]^{2-}$ and hints that $[Ph_4P]_2[Fe_4S_4(SEt)_3(NO)]$ is synthetically accessible (Figure S20). We also treated $(Ph_4P)_2[\mathbf{1\text{-}SEt}]$ with $(Ph_4P)NO_2$ and $PCy_3$, resulting in a partial conversion to $(Ph_4P)_2[\mathbf{1\text{-}NO}]$ (Figure S26). Given the similarities between $[\mathbf{1\text{-}SEt}]^{2-}$ and $[Fe_4S_4(SEt)_4]^{2-}$, the chelating nature of and structural rigidity conferred by $(tempS_3)^{3-}$ versus three $EtS^-$ donors or the donor strength differences between alkyl and aryl thiolates effectively controls extent of reaction toward nitrite in the presence of phosphines. Finally, reaction of $[Bu_4N]_2[Fe_2S_2Cl_4]$ with 4 equiv of $[Bu_4N][NO_2]$ and $PCy_3$ yields Roussin's black anion as an identifiable product in IR spectra (Figure S20).[64] Our findings demonstrate the broad applicability of nitrite sources and phosphines to effect reduction of nitrite to NO at synthetic FeS clusters.

From a mechanistic perspective, phosphines can serve as O atom acceptors or as reductants, the latter evident in prior reports where phosphines reduce $[Fe_4S_4]^{2+}$ clusters by one electron as in the synthesis of **2-Cl**.[55,57] Two possible mechanisms are cluster reduction followed by nitrite coordination and N−O bond scission or O atom transfer from a coordinated nitrite directly to the phosphine. To probe reduction or O atom transfer pathways, we reacted the synthetic NADH analog, 1-benzyl-1,4-dihydronicotinamide (BNAH), $[Et_3NH]Cl$, $[Ph_4P]NO_2$, and with **1-Cl**, which yielded $[\mathbf{1\text{-}NO}]^{2-}$ and $[Fe_4S_4(NO)_4]^{2-}$ based on IR and $^1$H NMR data of the product mixture (Figure S13, S21). Omission of $[Et_3NH]Cl$, BNAH, or nitrite from the reaction affords no nitrosylated cluster products based on IR spectroscopy. Thus, BNAH is competent to prime the $[Fe_4S_4]^{2+}$ cluster toward nitrite reductase reactivity, resulting in the nitrosylation of the cluster and cluster products indistinguishable from those generated with nitric oxide.[65,66]

Previously, FeS cluster nitrosylation was proposed as being NO dependent, reliant on the action of other enzymes on nitrite. Prior work examining the reactivity of nitrite toward FeS clusters were conducted *ex vivo* in the absence of reducing agents, which are available *in vivo*, or in cell studies wherein nitrite to NO reduction is also catalyzed by other cofactors.[24,51] Cellular concentrations of NADH are estimated in the $\mu$M range and elevated in cancer cell lines,[67] implying accessible conditions that mirror those in our reactions with BNAH, and that FeS nitrosylation by nitrite in the cellular environment is feasible. Moreover, our work demonstrates that nitrite and nitric oxide are both competent to trigger FeS cluster degradation in a strikingly similar manner and are both expected to activate the nitrosative stress response machinery. These outcomes call for a reexamination of nitrite as not only a store of the more biologically active nitric oxide but also an agent of nitrosative damage.

## ■ ASSOCIATED CONTENT

### Supporting Information

The Supporting Information is available free of charge at https://pubs.acs.org/doi/10.1021/jacs.5c05636.



https://doi.org/10.1021/jacs.5c05636
J. Am. Chem. Soc. XXXX, XXX, XXX−XXX

Materials and methods; supplementary figures, Figures S1−S25, Tables S1−S9 (crystallographic data), Mössbauer spectroscopy methods and analysis of temp-$(P^iPr_2)_3$ complexes; computational methods (PDF)

### Accession Codes

Deposition Numbers 2421475−2421476 and 2421478 contain the supplementary crystallographic data for this paper. These data can be obtained free of charge via the joint Cambridge Crystallographic Data Centre (CCDC) and Fachinformationszentrum Karlsruhe Access Structures service.

## AUTHOR INFORMATION


### Corresponding Authors

**Leslie J. Murray** − *Center for Catalysis and Florida Center for Heterocyclic Chemistry, Department of Chemistry, University of Florida, Gainesville, Florida 32611, United States;* orcid.org/0000-0002-1568-958X; Email: murray@chem.ufl.edu

**Ricardo García-Serres** − *Université Grenoble Alpes, CNRS, CEA, BIG, LCBM (UMR 5249), F-38054 Grenoble, France;* orcid.org/0000-0001-5203-0568; Email: ricardo.garcia@cea.fr

### Authors

**Subhadeep Bera** − *Center for Catalysis and Florida Center for Heterocyclic Chemistry, Department of Chemistry, University of Florida, Gainesville, Florida 32611, United States*

**Arijeet Ghude** − *Center for Catalysis and Florida Center for Heterocyclic Chemistry, Department of Chemistry, University of Florida, Gainesville, Florida 32611, United States*

**Vincent J. Catalano** − *Department of Chemistry, University of Nevada, Reno, Nevada 89557, United States;* orcid.org/0000-0003-2151-2892

**Jean-Marie Mouesca** − *Université Grenoble Alpes, CNRS, CEA/IRIG-SyMMES, F-38054 Grenoble, France;* orcid.org/0000-0001-7497-1430

Complete contact information is available at: https://pubs.acs.org/10.1021/jacs.5c05636


### Author Contributions

The manuscript was written through contributions of all authors. All authors have given approval to the final version of the manuscript.

### Notes

The authors declare no competing financial interest.

## ACKNOWLEDGMENTS

We acknowledge Dr. Ł. Dobrzycki for assistance with single crystal XRD measurements at the University of Florida, and funding from the National Science Foundation (CHE-2102098) and National Institutes of Health (R01-GM123241). X-ray diffractometers for measurements at the Center for X-ray Crystallography at UF were supported by the National Science Foundation (CHE-1828064). Mass spectrometry data were collected on instrumentation supported by the National Institutes of Health (S10 OD021758-01A1 and S10 OD030250-01A1). R.G.S. thanks Labex Arcane, CBH-EUR-GS (ANR-17-EURE-0003) for financial support.

## REFERENCES


(1) Ohshima, H.; Tatemichi, M.; Sawa, T. Chemical Basis of Inflammation-Induced Carcinogenesis. *Arch. Biochem. Biophys.* **2003**, *417* (1), 3−11.

(2) Patel, R. P.; McAndrew, J.; Sellak, H.; White, C. R.; Jo, H.; Freeman, B. A.; Darley-Usmar, V. M. Biological Aspects of Reactive Nitrogen Species. *Biochim. Biophys. Acta - Bioenerg.* **1999**, *1411* (2), 385−400.

(3) Li, C.-Q.; Wogan, G. N. Nitric Oxide as a Modulator of Apoptosis. *Cancer Lett.* **2005**, *226* (1), 1−15.

(4) Li, C.-Q.; Pang, B.; Kiziltepe, T.; Trudel, L. J.; Engelward, B. P.; Dedon, P. C.; Wogan, G. N. Threshold Effects of Nitric Oxide-Induced Toxicity and Cellular Responses in Wild-Type and P53-Null Human Lymphoblastoid Cells. *Chem. Res. Toxicol.* **2006**, *19* (3), 399−406.

(5) Delledonne, M.; Zeier, J.; Marocco, A.; Lamb, C. Signal Interactions between Nitric Oxide and Reactive Oxygen Intermediates in the Plant Hypersensitive Disease Resistance Response. *Proc. Natl. Acad. Sci. U. S. A.* **2001**, *98* (23), 13454−13459.

(6) Culotta, E.; Koshland, D. E. NO News Is Good News. *Science* **1992**, *258* (5090), 1862−1865.

(7) Gow, A. J.; Ischiropoulos, H. Nitric Oxide Chemistry and Cellular Signaling. *J. Cell. Physiol.* **2001**, *187* (3), 277−282.

(8) Snyder, S. H. Nitric Oxide: First in a New Class of Neurotransmitters. *Science* **1992**, *257* (5069), 494−496.

(9) Kelm, M. Nitric Oxide Metabolism and Breakdown. *Biochim. Biophys. Acta - Bioenerg.* **1999**, *1411* (2), 273−289.

(10) Thomas, D. D.; Ridnour, L. A.; Isenberg, J. S.; Flores-Santana, W.; Switzer, C. H.; Donzelli, S.; Hussain, P.; Vecoli, C.; Paolocci, N.; Ambs, S.; Colton, C. A.; Harris, C. C.; Roberts, D. D.; Wink, D. A. The Chemical Biology of Nitric Oxide: Implications in Cellular Signaling. *Free Radic. Biol. Med.* **2008**, *45* (1), 18−31.

(11) Andrabi, S. M.; Sharma, N. S.; Karan, A.; Shahriar, S. M. S.; Cordon, B.; Ma, B.; Xie, J. Nitric Oxide: Physiological Functions, Delivery, and Biomedical Applications. *Adv. Sci.* **2023**, *10* (30), No. 2303259.

(12) Fülöp, V.; Moir, J. W. B.; Ferguson, S. J.; Hajdu, J. The Anatomy of a Bifunctional Enzyme: Structural Basis for Reduction of Oxygen to Water and Synthesis of Nitric Oxide by Cytochrome Cd1. *Cell* **1995**, *81* (3), 369−377.

(13) Baker, S. C.; Saunders, N. F. W.; Willis, A. C.; Ferguson, S. J.; Hajdu, J.; Fülöp, V. Cytochrome *Cd*1 Structure: Unusual Haem Environments in a Nitrite Reductase and Analysis of Factors Contributing to $\beta$-Propeller Folds1. *J. Mol. Biol.* **1997**, *269* (3), 440−455.

(14) Cheesman, M. R.; Ferguson, S. J.; Moir, J. W. B.; Richardson, D. J.; Zumft, W. G.; Thomson, A. J. Two Enzymes with a Common Function but Different Heme Ligands in the Forms as Isolated. Optical and Magnetic Properties of the Heme Groups in the Oxidized Forms of Nitrite Reductase, Cytochrome Cd1, from Pseudomonas Stutzeri and Thiosphaera Pantotropha. *Biochemistry* **1997**, *36* (51), 16267−16276.

(15) Williams, P. A.; Fülöp, V.; Garman, E. F.; Saunders, N. F. W.; Ferguson, S. J.; Hajdu, J. Haem-Ligand Switching during Catalysis in Crystals of a Nitrogen-Cycle Enzyme. *Nature* **1997**, *389* (6649), 406−412.

(16) Jafferji, A.; Allen, J. W. A.; Ferguson, S. J.; Fülöp, V. X-Ray Crystallographic Study of Cyanide Binding Provides Insights into the Structure-Function Relationship for Cytochrome*Cd* 1 Nitrite Reductase from *Paracoccus Pantotrophus* *. *J. Biol. Chem.* **2000**, *275* (33), 25089−25094.

(17) Maia, L. B.; Moura, J. J. G. How Biology Handles Nitrite. *Chem. Rev.* **2014**, *114* (10), 5273−5357.

(18) O'Shea, S. K.; Wang, W.; Wade, R. S.; Castro, C. E. Selective Oxygen Transfers with Iron(III) Porphyrin Nitrite. *J. Org. Chem.* **1996**, *61* (18), 6388−6395.

(19) Heinecke, J. L.; Khin, C.; Pereira, J. C. M.; Suárez, S. A.; Iretskii, A. V.; Doctorovich, F.; Ford, P. C. Nitrite Reduction

Mediated by Heme Models. Routes to NO and HNO? *J. Am. Chem. Soc.* **2013**, *135* (10), 4007−4017.
(20) Patra, A. K.; Afshar, R. K.; Rowland, J. M.; Olmstead, M. M.; Mascharak, P. K. Thermally Induced Stoichiometric and Catalytic O-Atom Transfer by a Non-Heme Iron(III)−Nitro Complex: First Example of Reversible $\{Fe-NO\}^7 \leftrightarrow Fe^{III}$-$NO_2$ Transformation in the Presence of Dioxygen. *Angew. Chem., Int. Ed.* **2003**, *42* (37), 4517−4521.
(21) Afshar, R. K.; Eroy-Reveles, A. A.; Olmstead, M. M.; Mascharak, P. K. Stoichiometric and Catalytic Secondary O-Atom Transfer by Fe(III)−$NO_2$ Complexes Derived from a Planar Tetradentate Non-Heme Ligand: Reminiscence of Heme Chemistry. *Inorg. Chem.* **2006**, *45* (25), 10347−10354.
(22) Ching, W.-M.; Hung, C.-H. Interior Aliphatic C−H Bond Activation on Iron(II) N-Confused Porphyrin through Synergistic Nitric Oxide Binding and Iron Oxidation. *Chem. Commun.* **2012**, *48* (41), 4989−4991.
(23) Ching, W.-M.; Chen, P. P.-Y.; Hung, C.-H. A Mechanistic Study of Nitrite Reduction on Iron(II) Complexes of Methylated N-Confused Porphyrins. *Dalton Trans.* **2017**, *46* (43), 15087−15094.
(24) Crack, J. C.; Balasiny, B. K.; Bennett, S. P.; Rolfe, M. D.; Froes, A.; MacMillan, F.; Green, J.; Cole, J. A.; Le Brun, N. E. The Di-Iron Protein YtfE Is a Nitric Oxide-Generating Nitrite Reductase Involved in the Management of Nitrosative Stress. *J. Am. Chem. Soc.* **2022**, *144* (16), 7129−7145.
(25) Nunoshiba, T.; deRojas-Walker, T.; Wishnok, J. S.; Tannenbaum, S. R.; Demple, B. Activation by Nitric Oxide of an Oxidative-Stress Response That Defends Escherichia Coli against Activated Macrophages. *Proc. Natl. Acad. Sci. U. S. A.* **1993**, *90* (21), 9993−9997.
(26) Wei, T.; Chen, C.; Hou, J.; Xin, W.; Mori, A. Nitric Oxide Induces Oxidative Stress and Apoptosis in Neuronal Cells. *Biochim. Biophys. Acta, Mol. Cell Res.* **2000**, *1498* (1), 72−79.
(27) Demple, B. Signal Transduction by Nitric Oxide in Cellular Stress Responses. *Mol. Cell. Biochem.* **2002**, *234* (1), 11−18.
(28) Cruz-Ramos, H.; Crack, J.; Wu, G.; Hughes, M. N.; Scott, C.; Thomson, A. J.; Green, J.; Poole, R. K. NO Sensing by FNR: Regulation of the Escherichia Coli NO-detoxifying Flavohaemoglobin, Hmp. *EMBO J.* **2002**, *21* (13), 3235−3244.
(29) Kudhair, B. K.; Hounslow, A. M.; Rolfe, M. D.; Crack, J. C.; Hunt, D. M.; Buxton, R. S.; Smith, L. J.; Le Brun, N. E.; Williamson, M. P.; Green, J. Structure of a Wbl Protein and Implications for NO Sensing by M. Tuberculosis. *Nat. Commun.* **2017**, *8* (1), 2280.
(30) Anand, K.; Tripathi, A.; Shukla, K.; Malhotra, N.; Jamithireddy, A. K.; Jha, R. K.; Chaudhury, S. N.; Rajmani, R. S.; Ramesh, A.; Nagaraja, V.; Gopal, B.; Nagaraju, G.; Narain Seshayee, A. S.; Singh, A. *Mycobacterium Tuberculosis* SufR Responds to Nitric Oxide via Its 4Fe−4S Cluster and Regulates Fe−S Cluster Biogenesis for Persistence in Mice. *Redox Biol.* **2021**, *46*, No. 102062.
(31) Crack, J. C.; den Hengst, C. D.; Jakimowicz, P.; Subramanian, S.; Johnson, M. K.; Buttner, M. J.; Thomson, A. J.; Le Brun, N. E. Characterization of [4Fe-4S]-Containing and Cluster-Free Forms of Streptomyces WhiD. *Biochemistry* **2009**, *48* (51), 12252−12264.
(32) Crack, J. C.; Munnoch, J.; Dodd, E. L.; Knowles, F.; Al Bassam, M. M.; Kamali, S.; Holland, A. A.; Cramer, S. P.; Hamilton, C. J.; Johnson, M. K.; Thomson, A. J.; Hutchings, M. I.; Le Brun, N. E. NsrR from Streptomyces Coelicolor Is a Nitric Oxide-Sensing [4Fe-4S] Cluster Protein with a Specialized Regulatory Function *. *J. Biol. Chem.* **2015**, *290* (20), 12689−12704.
(33) Volbeda, A.; Dodd, E. L.; Darnault, C.; Crack, J. C.; Renoux, O.; Hutchings, M. I.; Le Brun, N. E.; Fontecilla-Camps, J. C. Crystal Structures of the NO Sensor NsrR Reveal How Its Iron-Sulfur Cluster Modulates DNA Binding. *Nat. Commun.* **2017**, *8* (1), 15052.
(34) Rohac, R.; Crack, J. C.; de Rosny, E.; Gigarel, O.; Le Brun, N. E.; Fontecilla-Camps, J. C.; Volbeda, A. Structural Determinants of DNA Recognition by the NO Sensor NsrR and Related Rrf2-Type [FeS]-Transcription Factors. *Commun. Biol.* **2022**, *5* (1), 1−11.
(35) Crack, J. C.; Svistunenko, D. A.; Munnoch, J.; Thomson, A. J.; Hutchings, M. I.; Le Brun, N. E. Differentiated, Promoter-Specific Response of [4Fe-4S] NsrR DNA Binding to Reaction with Nitric Oxide *. *J. Biol. Chem.* **2016**, *291* (16), 8663−8672.
(36) Vanin, A. F.; Borodulin, R. R.; Mikoyan, V. D. Dinitrosyl Iron Complexes with Natural Thiol-Containing Ligands in Aqueous Solutions: Synthesis and Some Physico-Chemical Characteristics (A Methodological Review). *Nitric Oxide* **2017**, *66*, 1−9.
(37) Drapier, J.-C. Interplay between NO and [Fe-S] Clusters: Relevance to Biological Systems. *Methods* **1997**, *11* (3), 319−329.
(38) Foster, M. W.; Cowan, J. A. Chemistry of Nitric Oxide with Protein-Bound Iron Sulfur Centers. Insights on Physiological Reactivity. *J. Am. Chem. Soc.* **1999**, *121* (17), 4093−4100.
(39) Ekanger, L. A.; Oyala, P. H.; Moradian, A.; Sweredoski, M. J.; Barton, J. K. Nitric Oxide Modulates Endonuclease III Redox Activity by a 800 mV Negative Shift upon $[Fe_4S_4]$ Cluster Nitrosylation. *J. Am. Chem. Soc.* **2018**, *140* (37), 11800−11810.
(40) Crack, J. C.; Green, J.; Thomson, A. J.; Le Brun, N. E. Iron−Sulfur Cluster Sensor-Regulators. *Curr. Opin. Chem. Biol.* **2012**, *16* (1), 35−44.
(41) Harrop, T. C.; Tonzetich, Z. J.; Reisner, E.; Lippard, S. J. Reactions of Synthetic [2Fe-2S] and [4Fe-4S] Clusters with Nitric Oxide and Nitrosothiols. *J. Am. Chem. Soc.* **2008**, *130* (46), 15602−15610.
(42) Victor, E.; Lippard, S. J. A Tetranitrosyl [4Fe−4S] Cluster Forms En Route to Roussin's Black Anion: Nitric Oxide Reactivity of $[Fe_4S_4(LS_3)L']^{2-}$. *Inorg. Chem.* **2014**, *53* (10), 5311−5320.
(43) Tonzetich, Z. J.; Do, L. H.; Lippard, S. J. Dinitrosyl Iron Complexes Relevant to Rieske Cluster Nitrosylation. *J. Am. Chem. Soc.* **2009**, *131* (23), 7964−7965.
(44) Tran, C. T.; Kim, E. Acid-Dependent Degradation of a [2Fe−2S] Cluster by Nitric Oxide. *Inorg. Chem.* **2012**, *51* (19), 10086−10088.
(45) Oakley, K. M.; Zhao, Z.; Lehane, R. L.; Ma, J.; Kim, E. Generation of H2S from Thiol-Dependent NO Reactivity of Model [4Fe-4S] Cluster and Roussin's Black Anion. *Inorg. Chem.* **2021**, *60* (21), 15910−15917.
(46) Tsai, F.-T.; Chiou, S.-J.; Tsai, M.-C.; Tsai, M.-L.; Huang, H.-W.; Chiang, M.-H.; Liaw, W.-F. Dinitrosyl Iron Complexes (DNICs) $[L_2Fe(NO)_2]^-$ (L = Thiolate): Interconversion among $\{Fe(NO)_2\}^9$ DNICs, $\{Fe(NO)_2\}^{10}$ DNICs, and [2Fe-2S] Clusters, and the Critical Role of the Thiolate Ligands in Regulating NO Release of DNICs. *Inorg. Chem.* **2005**, *44* (16), 5872−5881.
(47) Kim, Y.; Sridharan, A.; Suess, D. L. M. The Elusive Mononitrosylated $[Fe_4S_4]$ Cluster in Three Redox States. *Angew. Chem., Int. Ed.* **2022**, *61* (47), No. e202213032.
(48) Serrano, P. N.; Wang, H.; Crack, J. C.; Prior, C.; Hutchings, M. I.; Thomson, A. J.; Kamali, S.; Yoda, Y.; Zhao, J.; Hu, M. Y.; Alp, E. E.; Oganesyan, V. S.; Le Brun, N. E.; Cramer, S. P. Nitrosylation of Nitric-Oxide-Sensing Regulatory Proteins Containing [4Fe-4S] Clusters Gives Rise to Multiple Iron−Nitrosyl Complexes. *Angew. Chem., Int. Ed.* **2016**, *55* (47), 14575−14579.
(49) Crack, J. C.; Smith, L. J.; Stapleton, M. R.; Peck, J.; Watmough, N. J.; Buttner, M. J.; Buxton, R. S.; Green, J.; Oganesyan, V. S.; Thomson, A. J.; Le Brun, N. E. Mechanistic Insight into the Nitrosylation of the [4Fe−4S] Cluster of WhiB-like Proteins. *J. Am. Chem. Soc.* **2011**, *133* (4), 1112−1121.
(50) Crack, J. C.; Stapleton, M. R.; Green, J.; Thomson, A. J.; Le Brun, N. E. Mechanism of $[4Fe-4S](Cys)_4$ Cluster Nitrosylation Is Conserved among NO-Responsive Regulators. *J. Biol. Chem.* **2013**, *288* (16), 11492−11502.
(51) Weigel, J. A.; Holm, R. H. Intrinsic Binding Properties of a Differentiated Iron Subsite in Analogs of Native $[Fe_4S_4]^{2+}$ Clusters. *J. Am. Chem. Soc.* **1991**, *113* (11), 4184−4191.
(52) Terada, T.; Wakimoto, T.; Nakamura, T.; Hirabayashi, K.; Tanaka, K.; Li, J.; Matsumoto, T.; Tatsumi, K. Tridentate Thiolate Ligands: Application to the Synthesis of the Site-Differentiated [4Fe-4S] Cluster Having a Hydrosulfide Ligand at the Unique Iron Center. *Chem.—Asian J.* **2012**, *7* (5), 920−929.


https://doi.org/10.1021/jacs.5c05636
J. Am. Chem. Soc. XXXX, XXX, XXX−XXX

(53) Dodd, E. L.; Le Brun, N. E. Probing the Mechanism of the Dedicated NO Sensor [4Fe-4S] NsrR: The Effect of Cluster Ligand Environment. *J. Inorg. Biochem.* **2024**, *252*, No. 112457.
(54) Noodleman, L. Exchange Coupling and Resonance Delocalization in Reduced Iron-Sulfur $[Fe_4S_4]^+$ and Iron-Selenium $[Fe_4Se_4]^+$ Clusters. 1. Basic Theory of Spin-State Energies and EPR and Hyperfine Properties. *Inorg. Chem.* **1991**, *30* (2), 246−256.
(55) Deng, L.; Majumdar, A.; Lo, W.; Holm, R. H. Stabilization of 3:1 Site-Differentiated Cubane-Type Clusters in the $[Fe_4S_4]^{1+}$ Core Oxidation State by Tertiary Phosphine Ligation: Synthesis, Core Structural Diversity, and S = 1/2 Ground States. *Inorg. Chem.* **2010**, *49* (23), 11118−11126.
(56) Grunwald, L.; Clémancey, M.; Klose, D.; Dubois, L.; Gambarelli, S.; Jeschke, G.; Wörle, M.; Blondin, G.; Mougel, V. A Complete Biomimetic Iron-Sulfur Cubane Redox Series. *Proc. Natl. Acad. Sci. U. S. A.* **2022**, *119* (31), No. e2122677119.
(57) Goh, C.; Segal, B. M.; Huang, J.; Long, J. R.; Holm, R. H. Polycubane Clusters: Synthesis of $[Fe_4S_4(PR_3)_4]^{1+,0}$ (R = But, Cy, Pri) and $[Fe_4S_4]^0$ Core Aggregation upon Loss of Phosphine. *J. Am. Chem. Soc.* **1996**, *118* (47), 11844−11853.
(58) Goh, C.; Holm, R. H. Synthesis and Structures of the Cuboidal Iron-Sulfur-Nitrosyl-Phosphine Clusters $[Fe_4S_3(NO)_4(PR_3)_3]^{0,1+}$ (R = Et, $Pr^i$, $C_6H_{11}$). *Inorg. Chim. Acta* **1998**, *270* (1), 46−54.
(59) Brown, A. C.; Suess, D. L. M. Controlling Substrate Binding to $Fe_4S_4$ Clusters through Remote Steric Effects. *Inorg. Chem.* **2019**, *58* (8), 5273−5280.
(60) Le, L. N. V.; Joyce, J. P.; Oyala, P. H.; DeBeer, S.; Agapie, T. Highly Activated Terminal Carbon Monoxide Ligand in an Iron−Sulfur Cluster Model of FeMco with Intermediate Local Spin State at Fe. *J. Am. Chem. Soc.* **2024**, *146* (8), 5045−5050.
(61) Scott, A. G.; Agapie, T. Synthesis of a $Fe_3$−Carbyne Motif by Oxidation of an Alkyl Ligated Iron−Sulfur ($WFe_3S_3$) Cluster. *J. Am. Chem. Soc.* **2023**, *145* (1), 2−6.
(62) Scott, T. A.; Berlinguette, C. P.; Holm, R. H.; Zhou, H.-C. Initial Synthesis and Structure of an All-Ferrous Analogue of the Fully Reduced $[Fe_4S_4]^0$ Cluster of the Nitrogenase Iron Protein. *Proc. Natl. Acad. Sci. U. S. A.* **2005**, *102* (28), 9741−9744.
(63) Kalyvas, H.; Coucouvanis, D. Synthesis and Reactivity of a New Octanuclear Iron−Sulfur Nitrosyl Cluster. *Inorg. Chem.* **2006**, *45* (21), 8462−8464.
(64) Tsou, C.-C.; Lin, Z.-S.; Lu, T.-T.; Liaw, W.-F. Transformation of Dinitrosyl Iron Complexes $[(NO)_2Fe(SR)_2]^-$ (R = Et, Ph) into [4Fe-4S] Clusters $[Fe_4S_4(SPh)_4]^{2-}$: Relevance to the Repair of the Nitric Oxide-Modified Ferredoxin [4Fe-4S] Clusters. *J. Am. Chem. Soc.* **2008**, *130* (50), 17154−17160.
(65) Unden, G.; Bongaerts, J. Alternative Respiratory Pathways of *Escherichia Coli*: Energetics and Transcriptional Regulation in Response to Electron Acceptors. *Biochim. Biophys. Acta - Bioenerg.* **1997**, *1320* (3), 217−234.
(66) Belenky, P.; Bogan, K. L.; Brenner, C. $NAD^+$ Metabolism in Health and Disease. *Trends Biochem. Sci.* **2007**, *32* (1), 12−19.
(67) Yu, Q.; Heikal, A. A. Two-Photon Autofluorescence Dynamics Imaging Reveals Sensitivity of Intracellular NADH Concentration and Conformation to Cell Physiology at the Single-Cell Level. *J. Photochem. Photobiol., B* **2009**, *95* (1), 46−57.


https://doi.org/10.1021/jacs.5c05636
*J. Am. Chem. Soc.* XXXX, XXX, XXX−XXX